



TITLE:

Discovery of a Long-duration Superflare on a Young Solar-type Star EK Draconis with Nearly Similar Time Evolution for H alpha and White-light Emissions

AUTHOR(S):

Namekata, Kosuke; Maehara, Hiroyuki; Honda, Satoshi; Notsu, Yuta; Okamoto, Soshi; Takahashi, Jun; Takayama, Masaki; ... Isogai, Keisuke; Nogami, Daisaku; Shibata, Kazunari

CITATION:

Namekata, Kosuke ...[et al]. Discovery of a Long-duration Superflare on a Young Solar-type Star EK Draconis with Nearly Similar Time Evolution for H alpha and White-light Emissions. *The Astrophysical Journal Letters* 2022, 926(1): L5.

ISSUE DATE:

2022-02-10

URL:




<http://hdl.handle.net/2433/281947>

RIGHT:

© 2022. The Author(s). Published by the American Astronomical Society.; Original content from this work may be used under the terms of the Creative Commons Attribution 4.0 licence. Any further distribution of this work must maintain attribution to the author(s) and the title of the work, journal citation and DOI.



Discovery of a Long-duration Superflare on a Young Solar-type Star EK Draconis with Nearly Similar Time Evolution for H α and White-light Emissions

Kosuke Namekata^{1,2,3} , Hiroyuki Maehara⁴ , Satoshi Honda⁵, Yuta Notsu^{6,7,8} , Soshi Okamoto³, Jun Takahashi⁵, Masaki Takayama⁵, Tomohito Ohshima⁵, Tomoki Saito⁵, Noriyuki Katoh^{5,9}, Miyako Tozuka⁵, Katsuhiko L. Murata¹⁰, Futa Ogawa¹⁰, Masafumi Niwano¹⁰, Ryo Adachi¹⁰, Motoki Oeda¹⁰, Kazuki Shiraishi¹⁰, Keisuke Isogai^{3,11}, Daisaku Nogami³, and Kazunari Shibata^{12,13}

¹ ALMA Project, NAOJ, NINS, Osawa, Mitaka, Tokyo, 181-8588, Japan

² Department of Astronomy, Kyoto University, Sakyo, Kyoto 606-8502, Japan

³ Astronomical Observatory, Kyoto University, Sakyo, Kyoto 606-8502, Japan

⁴ Okayama Branch Office, Subaru Telescope, NAOJ, NINS, Kamogata, Asakuchi, Okayama 719-0232, Japan

⁵ Nishi-Harima Astronomical Observatory, Center for Astronomy, University of Hyogo, Sayo, Hyogo 679-5313, Japan

⁶ Laboratory for Atmospheric and Space Physics, University of Colorado Boulder, 3665 Discovery Drive, Boulder, CO 80303, USA

⁷ National Solar Observatory, 3665 Discovery Drive, Boulder, CO 80303, USA

⁸ Department of Earth and Planetary Sciences, Tokyo Institute of Technology, 2-12-1 Ookayama, Meguro-ku, Tokyo 152-8551, Japan

⁹ Graduate School of Human Development and Environment, Kobe University, 3-11 Tsurukabuto, Nada-ku, Kobe 657-8501, Japan

¹⁰ Department of Physics, Tokyo Institute of Technology, 2-12-1 Ookayama, Meguro-ku, Tokyo 152-8551, Japan

¹¹ Department of Multi-Disciplinary Sciences, Graduate School of Arts and Sciences, The University of Tokyo, Komaba, Meguro-ku, Tokyo 153-0041, Japan

¹² Kwasan Observatory, Kyoto University, Yamashina, Kyoto 607-8471, Japan

¹³ School of Science and Engineering, Doshisha University, Kyotanabe, Kyoto 610-0321, Japan

Received 2021 December 24; revised 2022 January 21; accepted 2022 January 23; published 2022 February 15

Abstract

Young solar-type stars are known to show frequent “superflares,” which may severely influence the habitable worlds on young planets via intense radiation and coronal mass ejections. Here we report an optical spectroscopic and photometric observation of a long-duration superflare on the young solar-type star EK Draconis (50–120 Myr age) with the Seimei telescope and Transiting Exoplanet Survey Satellite. The flare energy 2.6×10^{34} erg and white-light flare duration 2.2 hr are much larger than those of the largest solar flares, and this is the largest superflare on a solar-type star ever detected by optical spectroscopy. The H α emission profile shows no significant line asymmetry, meaning no signature of a filament eruption, unlike the only previous detection of a superflare on this star. Also, it did not show significant line broadening, indicating that the nonthermal heating at the flare footpoints is not essential or that the footpoints are behind the limb. The time evolution and duration of the H α flare are surprisingly almost the same as those of the white-light flare, which is different from general M-dwarf (super-)flares and solar flares. This unexpected time evolution may suggest that different radiation mechanisms than general solar flares are predominant, such as: (1) radiation from (off-limb) flare loops and (2) re-radiation via radiative back-warming, in both of which the cooling timescales of flare loops could determine the timescales of H α and white light.

Unified Astronomy Thesaurus concepts: [Magnetic variable stars \(996\)](#); [Solar analogs \(1941\)](#); [Stellar phenomena \(1619\)](#); [Stellar flares \(1603\)](#); [Optical flares \(1166\)](#); [Spectroscopy \(1558\)](#)

1. Introduction

Solar and stellar flares are explosive phenomena on the surfaces observed from radio to X-rays (see Shibata & Magara 2011; Benz 2017, for review). They are thought to be caused by the conversion of magnetic energy into kinetic and thermal energy via magnetic reconnection. In the case of solar flares, coronal mass ejections (CMEs) as well as X-rays and extreme ultraviolet rays have severe impacts on the planetary magnetosphere (see Temmer 2021 for a review). Therefore, magnetic activities on central stars cannot be ignored when discussing planetary habitability and civilization.

The largest flare energy observed on our Sun is approximately 10^{32} erg (e.g., Emslie et al. 2012) and larger flares, called “superflares,” with more than 10^{33} erg, have never been reported in modern solar observations (e.g., Aulanier et al. 2013). In

recent years, however, observations of solar-type (G-type main-sequence) stars have provided some insight into whether the present-day Sun can produce superflares, or if the young Sun could have experienced superflares. Vigorous searches for stellar flares over the past 30 yr have revealed not only that rapidly rotating, young, solar-type stars show frequent superflares (age of ~ 100 Myr; Audard et al. 1999) but also that slowly rotating, old solar-type stars show superflares with low-occurrence frequencies (ages of several Gyr; Maehara et al. 2012; Shibayama et al. 2013; Notsu et al. 2019; Okamoto et al. 2021). These discoveries suggest that the young Sun could have produced frequent superflares affecting a young Earth’s environment and also suggest a possibility that superflares may occur even on the present-day moderate Sun. In these contexts, superflares on solar-type stars have received attention from the solar community (e.g., Aulanier et al. 2013; Shibata et al. 2013), planetary community (e.g., Airapetian et al. 2020), and historical and geophysical communities (e.g., Miyake et al. 2012; Hayakawa et al. 2017). However, the mechanism causing radiation and mass ejection from superflares, which is needed to

answer the above questions of interest, remains unknown. It can be unveiled, however, by spectroscopic or multi-wavelength observations, although this is rare for solar-type stars.

EK Draconis (EK Dra) is a young solar-type star with an age of 50–125 Myr. It has a Sun-like atmosphere with an effective temperature of 5560–5700 K, radius of $0.94 R_{\odot}$, and mass of $0.95 M_{\odot}$ (Waite et al. 2017; Şenavcı et al. 2021). It is rapidly rotating with a period of 2.77 days and exhibits frequent stellar flares, so it is considered a good target of flare observations (Audard et al. 1999; Ayres 2015; Namekata et al. 2021). One UV spectroscopic observation of the decay phase of a superflare on EK Dra has been reported using the Hubble Space Telescope (Ayres 2015), which had been the only example of a spectral line observation for solar-type stars before. Recently, on another solar-type star, H II 345 (G8V), simultaneous observations with Kepler Space Telescope and XMM-Newton have detected X-ray and white-light emission from a superflare (Guarcello et al. 2019).

Optical spectroscopic observations are also essential to capture chromospheric phenomena (accompanied by UV radiation) and filament/prominence eruptions (indirect evidence of CMEs; see Ichimoto & Kurokawa 1984; Kowalski et al. 2013; Namekata et al. 2020b; Maehara et al. 2021, for optical spectroscopic observations of solar and M-dwarf flares). Our previous study (Namekata et al. 2021) reported the first detection of the optical $H\alpha$ spectra of a superflare of $\sim 10^{33}$ erg on the young solar-type star EK Dra. Surprisingly, the $H\alpha$ spectra show a blueshifted absorption as evidence of a filament eruption, which has dramatically advanced our understanding. However, the mechanism of superflare radiation is still unknown because in the first event by Namekata et al. (2021), the flare emission was short-lived (~ 16 minutes) and had not been thoroughly investigated. In this Letter, we report detection of the optical spectra of another gigantic superflare event on EK Dra, which enables us to investigate the radiation mechanism. We show our observational summary in Section 2, results in Section 3, and discussion in Section 4.

2. Observations and Analysis

We conducted optical spectroscopic and photometric monitoring observations of the young solar-type star EK Dra from 2020 February to 2020 April. The spectroscopic data were obtained by the 3.8 m Seimei telescope (Kurita et al. 2020; see Section 2.2) and photometric data were obtained by the Transiting Exoplanet Survey Satellite (TESS; Ricker et al. 2015; see Section 2.1). Through this campaign, we succeeded in obtaining optical spectroscopic data of two superflares on the solar-type star, simultaneously with TESS photometry. One event on 2020 April 5 was already reported by Namekata et al. (2021), and another event on 2020 March 14 will be reported in this Letter.

2.1. TESS

TESS observed EK Dra (TIC 159613900) in sectors 14–16 (2019 July 18–2019 October 6) and 21–23 (2020 January 21–2020 April 15). EK Dra was observed with the 2 minute time cadence during this period (Ricker et al. 2015; Fausnaugh 2020). The TESS light curves are shown in Figure 1.

We performed automatic flare detection as follows (see, Maehara et al. 2021). We analyzed the TESS Pre-search Data

Conditioned Simple Aperture Photometry (PDC-SAP) light curves retrieved from the MAST Portal site (<https://mast.stsci.edu/portal/Mashup/Clients/Mast/Portal.html>). We first removed background rotational brightness variations using a fast Fourier transformation with a low-pass filter. We used the cutoff frequency of 3.0 day^{-1} in the first process. As the flare candidate, we selected the data points with the following criteria: (1) the peak residual brightness of the data point is higher than five times the TESS photometric errors, and (2) at least two consecutive data points exceed the three times the TESS photometric errors. A complex flare having multiple peaks was manually recognized as a single flare. Also, for flares of particular interest, we manually modeled the background component after removing the flare periods and changed the cutting frequency in the low-pass filter (for Figure 2(A), we use a cutting frequency of 10 day^{-1}).

In addition, we analyzed the TESS pixel-level data. No centroid motions are found during the superflares, which suggests it is associated with the stellar system rather than an instrumental systematic error or contamination from scattered background light or a distant star. Following the method of Shibayama et al. (2013), the white-light flare’s bolometric energy is derived by assuming the flaring spectra of 10,000 K blackbody radiation and TESS response function (Ricker et al. 2015).

2.2. 3.8 m Seimei Telescope

We introduce the utilization of low-resolution spectroscopic data from KOOLS-IFU (Kyoto Okayama Optical Low-dispersion Spectrograph with optical-fiber Integral Field Unit; Matsubayashi et al. 2019) installed at the 3.8 m Seimei Telescope (Kurita et al. 2020) at Okayama Observatory of Kyoto University. KOOLS-IFU is an optical spectrograph with a spectral resolution of $R \sim 2000$ covering a wavelength range from 5800–8000 Å, including the $H\alpha$ line (6562.8 Å).

The observation was conducted between 2020 February to April (TESS Sector 21–23), and the observational periods are indicated with blue color in Figure 1(C). The exposure time was set to be 30 s for these nights. The data reduction follows the prescription in Namekata et al. (2020b, 2021) with IRAF and PyRAF packages. Only the data of particular interest are shown in Figure 2. The original flare and template pre-flare $H\alpha$ spectra are shown in Figure 3. We measure the $H\alpha$ equivalent width (hereafter “EW,” which is an $H\alpha$ emission integrated for $6562.8-10 \text{ \AA} \sim 6562.8+10 \text{ \AA}$ after being normalized by the nearby continuum level) and plotted the light curve in Figure 2. For the flare data, the $H\alpha$ radiated energy is calculated by multiplying the enhanced $H\alpha$ EW by the continuum flux and integrating in time. The continuum flux of EK Dra around $H\alpha$ is derived as $1.57 \text{ W m}^{-2} \text{ nm}^{-1}$ at 1 au with the stellar distance given by Gaia Data Release 2 (Lindgren et al. 2018).

3. Results

3.1. Statistical Properties of White-light Flares on EK Dra Detected by TESS

Figure 1(A) and (C) show the TESS light curves observed in Sectors 14–16 and 21–23, respectively. Figure 1(B) and (D) show the detrended light curves for panels (A) and (C), respectively. We detected 94 flares on EK Dra in total, and the automatically detected flares are shown in red. Figure 1(E) shows the flare occurrence frequency as a function of flare

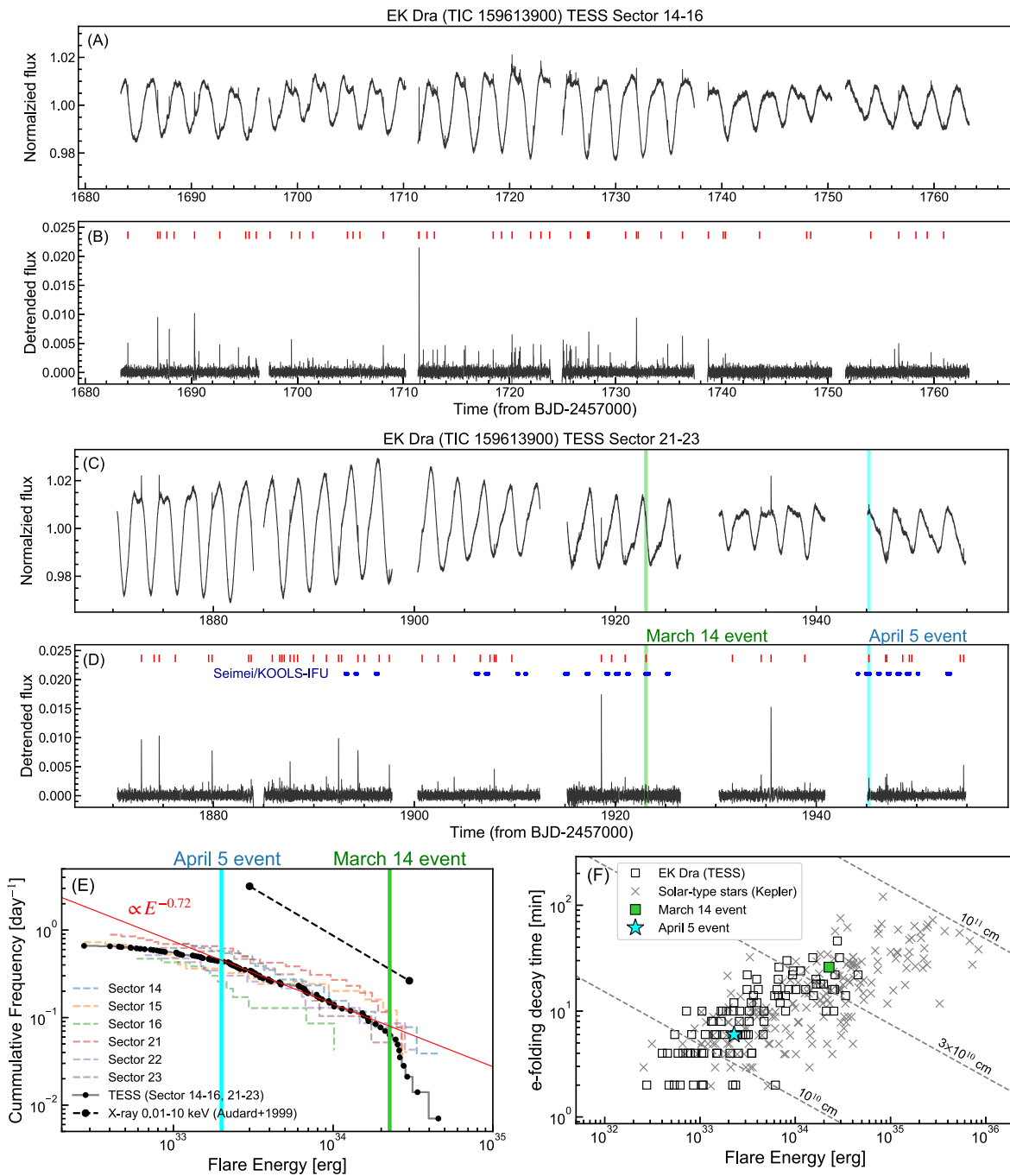


Figure 1. Superflares on EK Dra detected by TESS (Sector 14–16 and Sector 21–23). (A) The TESS light curve of Sector 14–16 (2019 July 18–2019 October 7) normalized by the average flux. (B) The detrended light curve of the panel (A). The times of the automatically detected flares are indicated by red lines. (C) The TESS light curve during Sector 21–23 (2020 January 21–2020 April 15) normalized by the average flux. (D) The detrended light curve of the panel (C). The periods of the monitoring observations by the Seimei telescope/KOOLS-IFU are shown in blue. Flares detected by ground-based telescopes on 14 March 2020 (this Letter) and 5 April 2020 (Namekata et al. 2021) are also shown in green and cyan, respectively. Note that the detrended light curve is automatically obtained by a low-pass filter without removing the flares, and background subtraction is different from Figure 2(A) (see Section 2.1 for the analysis). (E) The flare frequency on EK Dra detected by TESS. The flare frequency of EK Dra in X-rays, as determined by Audard et al. (1999), is shown as a black line for reference. The red solid line corresponds to the fitted one ($N(>E) \propto E^{-0.72 \pm 0.01}$) for 2×10^{33} to 2×10^{34} erg. (F) The relationship between flare energy and duration as determined by TESS. The gray cross points are the relationship between energy and duration obtained by Kepler (Maehara et al. 2015). The theoretical scaling relation with constant flare loop length (10^{10} , 3×10^{10} , and 10^{11} cm) is shown by the dashed line (Namekata et al. 2017).

energy. The relation can be fitted as $N(>E) \propto E^{-0.72 \pm 0.01}$ for 2×10^{33} to 2×10^{34} erg. Note that the fitted energy range is limited because a higher energy range could be affected by the lack of the statistics and energy cutoff, and the lower energy range could be affected by the flare detection sensitivity (Aschwanden 2019; Maehara et al. 2021; Okamoto et al. 2021).

The occurrence frequency of superflares with an energy of $> 10^{33}$ erg is 0.56 events per day, and that with an energy of $> 10^{34}$ erg is 0.14 events per day. The flare occurrence frequency varies for each sector (Figure 1(E)), and it is reported that the variation of flare frequency is positively correlated with the spot filling factor (Supplementary Figure 2 in Namekata

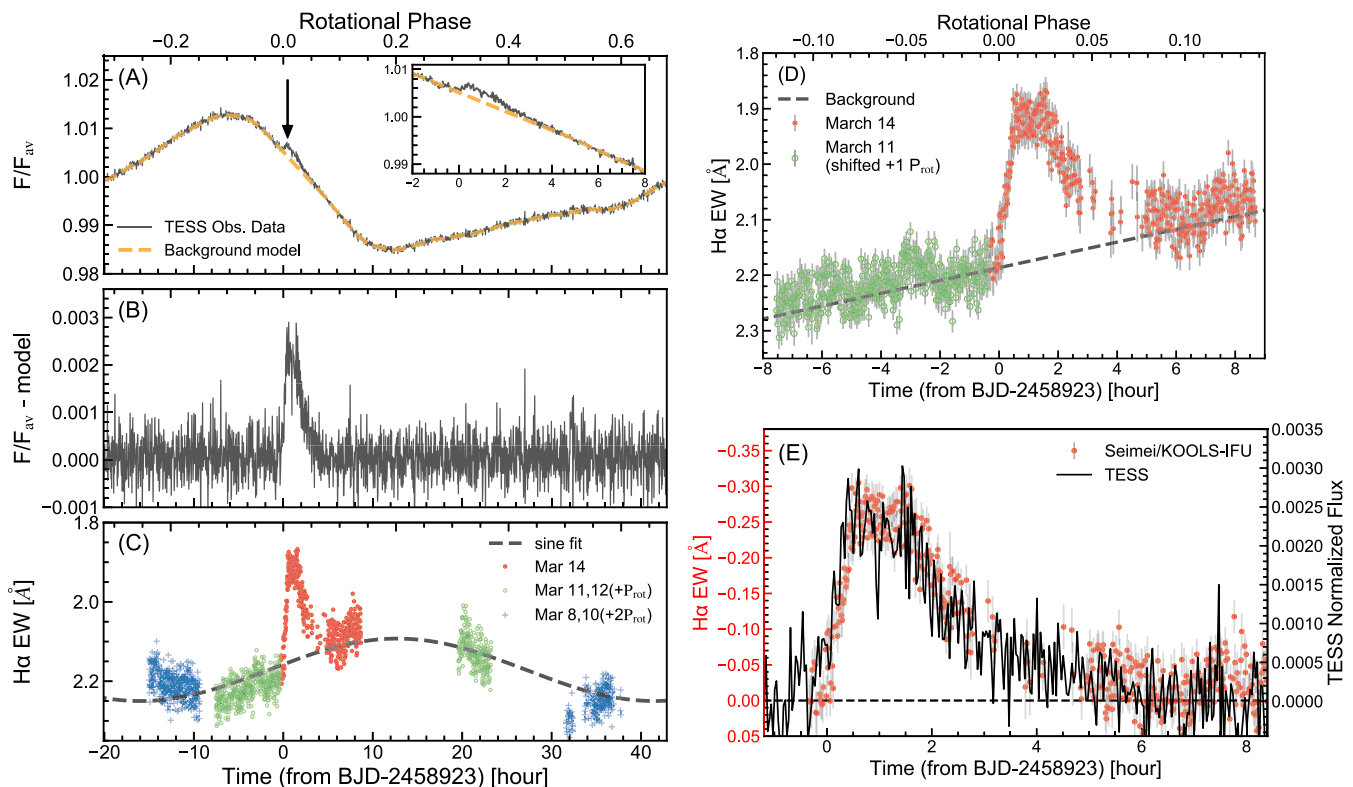


Figure 2. White light and $H\alpha$ light curves of the superflare and rotation variations on EK Dra observed on 2020 March 14. (A) The black line is the observed TESS light curve at the rotation phase when the superflare occurred. The orange dashed line is one fitted with the FFT and low-pass filter. The upper right in panel (A) is an enlarged light curve where the flare occurred. (B) The detrended TESS light curve (i.e., the black minus orange line in panel (A)). (C) The rotational modulation of the $H\alpha$ EW folded by the rotational period ($P_{\text{rot}} = 2.62$ days and $t_0 = \text{BJD}-2458923$). The different colors plot different rotational phases, and the red data are the rotation phase when the superflare occurred. The dashed line is a line fitted with a simple sine function for these rotation variations. The EW is the integrated $H\alpha$ absorption between 6552.8 and 6572.8 Å, normalized by the continuum level of 6517.8–6537.8 Å and 6587.8–6607.8 Å. (D) The $H\alpha$ light curve of the superflare (red) and its background level (black). The background model derived from the data on March 14 is consistent with the March 11 data. (E) The light curves of the superflare observed in $H\alpha$ (red) and TESS white light (black). The lack of $H\alpha$ data at approximately $\text{BJD}-2458923 + 4$ hr is due to the temporary cloud in the sky. The dashed line is the assumed background level for each.

et al. 2021). Also, note that the X-ray flare frequency of EK Dra of ~ 4.2 flares day^{-1} at 1995 (a dashed line in Figure 1(E) Audard et al. 1999) is much larger than the white-light flare frequency at 2019–2020. This can be caused by the long-term activity changes (e.g., 8.9 yr activity cycle is reported by Järvinen et al. 2018), or a difference in energy partition for X-ray and white-light emission (e.g., Kretzschmar 2011; Emslie et al. 2012).

Figure 1(F) shows the relationship between flare energy E_{flare} and decay time τ_{decay} on EK Dra observed by TESS ($\tau_{\text{decay}} \propto (E_{\text{flare}})^{0.49 \pm 0.04}$) and that on the solar-type stars observed by Kepler (with 1 minute cadence; Maehara et al. 2015). We found that the timescales of the EK Dra flares are comparable to those of the superflares in many solar-type stars discovered by Kepler.

3.2. The Gigantic $H\alpha$ and White-light Superflare on 2020 March 14

Figure 2(A) show the TESS white-light’s global light curves for a rotation phase of EK Dra around 2020 March 14. The period is derived as 2.62 days with a Lomb–Scargle periodogram (astropy.stats.LombScargle). The TESS light curve shows quasi-periodic brightness variations over the whole observational period, indicating a gigantic starspot on the star (Namekata et al. 2019, 2020a). As in the detrended light curve (Figure 2(B)), a white-light flare was detected by TESS on

BJD-2458923 (2020 March 14). The amplitude is approximately 0.3%, which is significantly larger than the TESS photometric errors (0.023%).

Simultaneously, we detected a clear $H\alpha$ flare (Figure 2(C)). There is a rotational brightness variation in $H\alpha$, anticorrelated with the white light. We consider that the $H\alpha$ modulation is due to the background stellar active region and then subtracted the background trend to extract the flare light curve. As in Figure 2(D), we have modeled the background by linearly fitting the pre-flare and post-flare levels of March 14 ($-0.4 \sim 0$ hr and $6 \sim 7$ hr) and obtained the flare light curve (Figure 2(E)).

The white-light flare energy (E_{WL}) is $(2.6 \pm 0.3) \times 10^{34}$ erg, and the $H\alpha$ energy ($E_{\text{H}\alpha}$) is $(4.0 \pm 0.4) \times 10^{32}$ erg (1.5% of the white-light energy); thus, it is classified as a superflare. This superflare is the ninth largest event in the six TESS sectors (Figure 1(E)). As in Figure 2(E), we found that the brightness evolution and timescales of the TESS white-light flare are almost the same as that of the $H\alpha$ flare. The FWHM of the white-light flare (t_{WL}) of and $H\alpha$ flare ($E_{\text{H}\alpha}$) is 2.2 hr and 2.3 hr, respectively.

Figure 3(A)–(C) shows the time evolution of the pre-flare-subtracted $H\alpha$ spectra. We could not find any significant asymmetry of $H\alpha$ line profiles and line broadening having higher velocity than the instrumental resolution of 150 km s^{-1} . Carefully looking at the spectra in Figure 4(A)–(D), however,

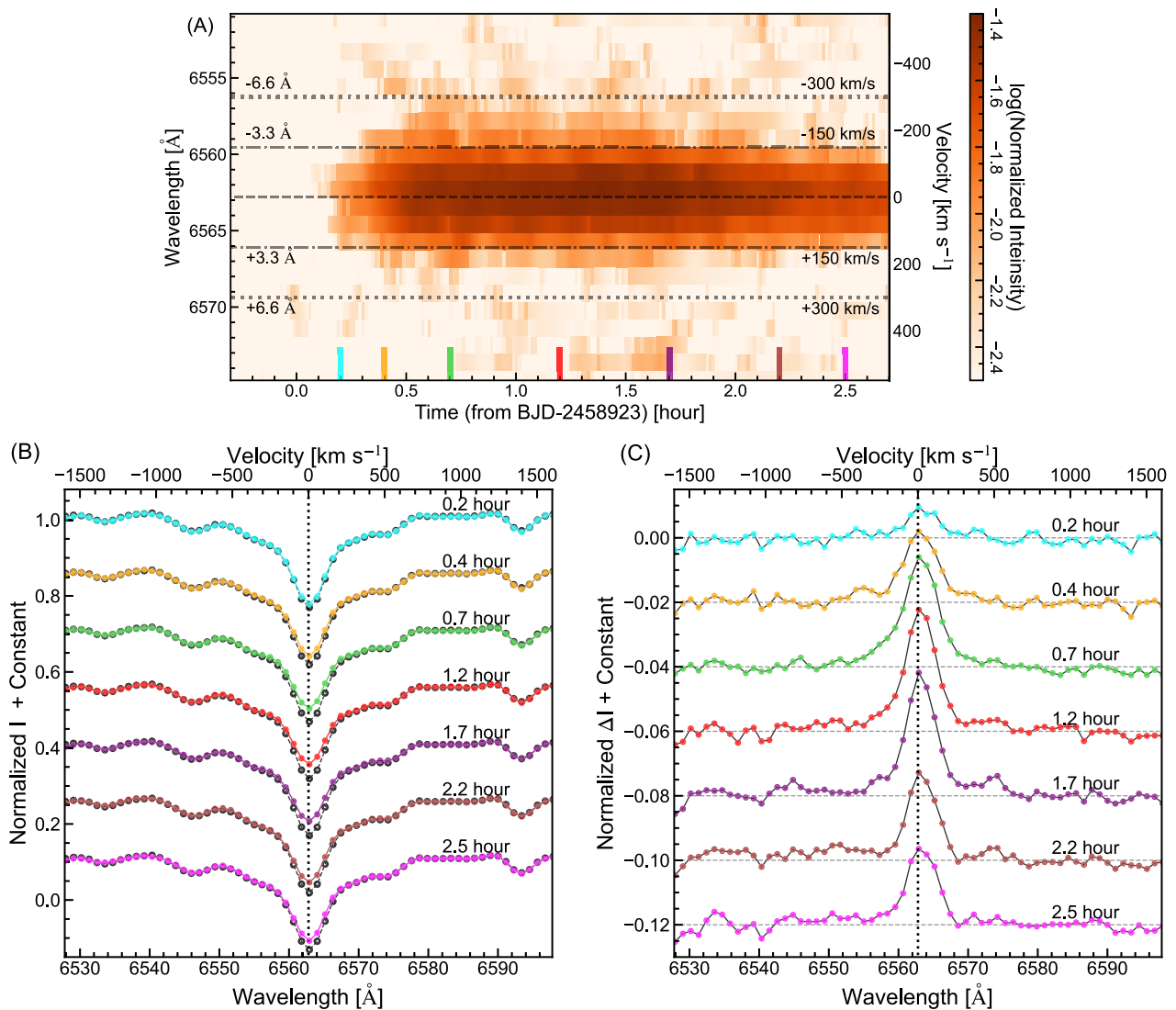


Figure 3. The temporal evolution of H α line profiles of the superflare on EK Dra. (A) Temporal variation of the pre-flare-subtracted H α spectra in the time-wavelength plane. The color bar shows the emission intensity normalized by the continuum level (6517.8–6537.8 Å and 6587.8–6607.8 Å). (B) The H α spectra of the superflare on 2020 March 14 observed with the Seimei Telescope/KOOLS-IFU. Each colored spectrum indicates the 20 minute averaged spectrum during the superflare with the central time indicated in the panel and the background black dashed line is the pre-flare template spectrum. The pre-flare template spectrum was created by averaging the first 35 pieces of data for the night (–0.35 hr to 0.15 hr in panel (A)). The spectra are normalized by the continuum level and the constant values are added for visibility. The dotted vertical line indicates the line center. (C) The pre-flare subtracted spectra of those in the panel (B). The basal level of each spectrum is plotted with the horizontal dashed line.

there may be a possible red asymmetry. The redshift velocity is approximately 20 km s^{-1} with a one-component fitting (Figure 3(A)–(B)), while it is approximately 100 km s^{-1} with a two-component fitting (Figure 4(C)–(D)). However, these are less than the instrumental dispersion velocity, and we would call this a “possible redshift” and limit ourselves to speculating its possibilities in this Letter.

4. Discussion

4.1. The Superflare on 2020 March 14 in Comparison with Solar and M-dwarf Flares

This section compares the superflare on March 14 with typical solar flares and M-dwarf (super-)flares. One of the significant differences between typical solar flares and the superflare on EK Dra is the value of energy and duration (see Table 1). The duration ~ 2.2 hr of the superflare with an energy

of 2.6×10^{34} erg is more than 10 times longer than those of solar white-light flares (1–10 minutes for 10^{29-31} erg; Namekata et al. 2017). The magnitude of these physical quantities is thought to attribute to the flare length scale. Namekata et al. (2017) proposed that the length scale (L) of solar and stellar flaring loops can be estimated from the white-light flare energy (E_{flare}) and the e-folding decay time of white-light flare (τ_{decay} of 26 minutes) based on the magnetic reconnection theory in the formula of

$$L \sim 1.64 \times 10^9 \left(\frac{\tau_{\text{decay}}}{100[\text{s}]} \right)^{2/5} \left(\frac{E_{\text{flare}}}{10^{30}[\text{erg}]} \right)^{1/5} [\text{cm}]. \quad (1)$$

This predicts the length scale as 3.8×10^{10} cm ($\sim 0.58 R_{\text{star}}$, R_{star} is stellar radius), which is much larger than the typical length scales of solar flares ($10^9 \sim 10^{10}$ cm).

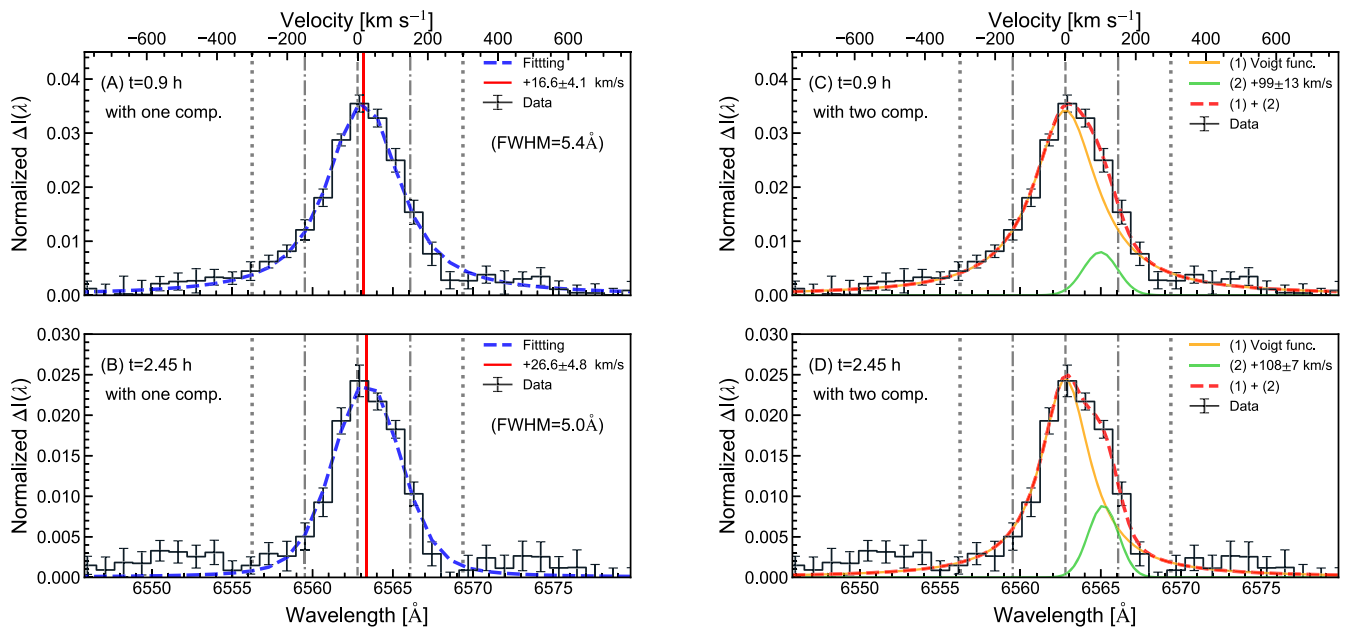


Figure 4. The $H\alpha$ line profiles of the superflare on EK Dra. (A, B) The pre-flare-subtracted $H\alpha$ spectra at $t = 0.9$ and 2.45 minutes, respectively. The blue lines result from the one component fitting with Voigt function. The red vertical lines correspond to the fitted line center. The line centers are $16.7 \pm 4.1 \text{ km s}^{-1}$ and $26.6 \pm 4.8 \text{ km s}^{-1}$, as indicated in each panel. The FWHM of the lines are 5.4 and 5.0 \AA , as also indicated in the panels. (C, D) The black data are the same as the panels (A) and (B), respectively. The colored line in the panels (C) and (D) are the results of two-component fitting with a Voigt function (orange line for the central component) and Gaussian function (green line for the redshift component). We first fitted the blue-wing profile with a Voigt function and fitted the residual of the red wing with the Gauss function. The red lines are the sum of the green and orange lines. The central velocity of the Gaussian (green lines) components of panels (C) and (D) are $99 \pm 13 \text{ km s}^{-1}$ and $108 \pm 7 \text{ km s}^{-1}$, respectively. The other properties of the red-wing enhancement are summarized in Table 1.

Furthermore, the most mysterious point is that the duration of $H\alpha$ and white light is approximately the same for the EK Dra superflare. In the case of solar flares (e.g., Hao et al. 2017, and see Table 1) and M-dwarf flares (e.g., Hawley & Pettersen 1991; Kowalski et al. 2013; Namekata et al. 2020b), the white light timescale is generally several times shorter than that of $H\alpha$. For example, the ratio of $H\alpha$ and white-light duration was reported as a factor of 2 in the 10^{33} erg class M-dwarf superflares by Namekata et al. (2020b). A much larger difference was reported for several M-dwarf flares by Kowalski et al. (2013). Possible mechanisms for this unexpected result of the EK Dra superflare will be discussed in Section 4.4.

In addition, the superflare did not show any significant line broadening synchronized with white-light emission (Figure 4), which is often seen in M-dwarf superflares (e.g., $\sim 14 \text{ \AA}$ for a 10^{33} erg class superflare in Namekata et al. 2020b) with the same spectrograph KOOLS-IFU. This indicates that high-energy electron heating is not essential for this superflare on EK Dra.

Other properties of stellar superflares can be explained by the analogy of solar and M-dwarf flares. The energy of $H\alpha$ relative to the energy of white light is roughly only a few percent for both EK Dra superflares (Table 1), and M-dwarf flares (e.g., Namekata et al. 2020b). In addition, the upper limits of the estimated values of the “possible” line asymmetry of $H\alpha$ line of this superflare do not contradict typical values of solar flares (see Table 1 and Ichimoto & Kurokawa 1984) even though they are real.

4.2. The Superflare on 2020 March 14 Compared with All Other Flares on EK Dra

In Figure 1(F), the relationship between flare energy and duration on EK Dra is compared with that on Kepler solar-type

stars. According to Namekata et al. (2017), the relationship for superflares on Kepler solar-type stars can be explained by the magnetic reconnection model (see, Equation (1)). Based on their theory, the consistency between EK Dra superflares and Kepler superflares means that the magnetic reconnection model can also be applied to the EK Dra superflares. Also, the superflare on March 14 is consistent with the majority of the flares on EK Dra, and this indicates that it was not a special case among other flares.

In Table 1, the superflare on EK Dra on 2020 March 14 is compared with that on 2020 April 5 reported by Namekata et al. (2021). The duration and white-light energy of superflare on 2020 March 14 is 10 times larger than those of the superflare on 2020 April 5. The significant difference between the March 14 and April 5 events is the association of the filament eruption signature (i.e., a blueshifted $H\alpha$ absorption as in Namekata et al. 2021). If a filament is in the front of the star and has a line-of-sight velocity, a blueshifted absorption should be observed (e.g., Namekata et al. 2021, and references therein). In other words, this result of March 14 event means that a filament eruption could occur either outside the stellar disk or perpendicular to the line of sight, meaning the flare could occur around the stellar limb (see the related discussion in Section 4.3 and 4.4). Other than these possibilities, the lack of a signature of filament eruption on March 14 may indicate that mass ejection events do not always happen for every superflare, as not all flares are accompanied by CMEs in the case of the Sun (e.g., Yashiro & Gopalswamy 2009).

4.3. Relation between the Superflare and Spot Groups

The anticorrelated rotational variation in $H\alpha$ and white light (Figure 2(A), (C)) is the same as the Sun-as-a-star active region modulation (e.g., Maldonado et al. 2019), indicating that the

Table 1
Summary of Properties of the Superflares on EK Dra and Solar Flares

	E_{WL} (erg)	t_{WL}	$E_{\text{H}\alpha}/E_{\text{WL}}$	$t_{\text{H}\alpha}/t_{\text{WL}}^{\text{a}}$	Asym. ^c	$I_{\text{red}}/I_{\text{cen}}^{\text{c}}$	V_{redshift} (km/s)	Reference
EK Dra (Mar 14)	2.6×10^{34}	2.2 hr ^d	0.015	1.1	No (Red)	(~0.36)	(~26.6 ^d /116 ^e)	This Letter
EK Dra (Apr 5) ^f	2.0×10^{33}	16 minutes ^b	(0.0085)	(1.1)	ref. ⁽¹⁾
The Sun	$10^{29-32(2,3)}$	1–10 minutes ^{b (3)}	...	$t_{\text{H}\alpha} > t_{\text{WL}}^{\text{(4)}}$	Red ^{g (5,6)}}	~several $\times 0.1^{\text{(5)}}$	$\leq 150^{\text{(5)}}$	ref. ^{(2–6)}}

Notes. “–” means no value and values in parentheses “()” are only reference values.

^a The FWHM duration of the flare.

^b The total duration of the flare.

^c “Red” means the red wind enhancement of the H α line emission profiles.

^d Single-component fitting.

^e Two-component fitting.

^f The flare emission on April 5 in Namekata et al. (2021) is very short-lived and its light curve is a combination of blueshift absorption and flaring emission. The H α flare duration is expected to be underestimated, and the line asymmetry of the H α flaring component was difficult to identify. Note that the blueshifted “absorption” in the flare on April 5 is not a flare radiation component, so the asymmetry is described here as “–”.

^g Ref.(5) reported that only 5% of solar flares show blue asymmetry and it is rare.

References. (1): Namekata et al. (2021). (2): Shibata & Magara (2011). (3): Namekata et al. (2017). (4): Hao et al. (2017). (5): Ichimoto & Kurokawa (1984). (6): Švestka et al. (1962).

chromosphere around the starspot (group) is magnetically heated and appears bright. The spot area on EK Dra estimated from the white-light brightness variation is 0.032 of the stellar disk by using the method of Maehara et al. (2017), and the length scale is 0.18 of R_{star} (1.2×10^{10} cm, in the photosphere), which is one-third of the flare loop length scale of $0.58 R_{\text{star}}$ (in the corona). The stored magnetic energy is roughly 1.2×10^{36} erg when the mean magnetic field is 1000 G (see Equation (1) in Shibata et al. 2013), meaning that the star had enough energy to produce the superflares.

The rotational modulation is not entirely symmetric in time (Figure 2(B)), suggesting the existence of multiple starspots (groups) rather than a single concentrated starspot. This superflare occurs at a +0.11 rotation period relative to the local maximum of the TESS light curve and at a –0.19 rotation period relative to the local minimum. This means that the flare occurred when a giant spot (group) started to be visible via stellar rotation. If we assume that the superflare occur around the dominant spot, the superflare can have occurred near the stellar limb. This may explain no signature of a filament eruption (Section 4.2).

4.4. Possible Emission Mechanisms

The most notable point of this superflare is that the duration and light curve evolution of H α are the same as those of white light as in Section 4.2. In the standard model of solar flares, white-light flares are emitted from the photosphere or/and chromosphere heated by nonthermal electrons, while H α is emitted mainly from both the nonthermally and thermally heated chromosphere (e.g., Shibata & Magara 2011; Kowalski et al. 2016). Since the timescale of thermal heating is, in general, longer than that of nonthermal heating, H α flares are thought to be qualitatively longer than white-light flares (see Table 1, the so-called *Neupert* effect; Neupert 1968). This standard model cannot explain the time evolution of the superflare on EK Dra. In addition, the lack of H α line broadening may indicate that nonthermal heating at the footpoints, a main flare driver in large solar flares (Aschwanden et al. 2017), is less dominant.

Then, what emission mechanism can explain the unexpected time evolution of the superflare? We propose the following two hypotheses: first, Nizamov (2019) proposed that the X-ray

back-warming can produce white-light enhancement in the photosphere in such an extreme case. Although the radiative back-warming is proposed as one contributor to white-light emission even for solar flares (e.g., Hao et al. 2017), its dominance is unknown. If this process can be applied, both white-light and H α emissions can last as long as the thermal emission in the coronal loop does. If the heated photosphere covers 10% of the stellar disk (~the square of the length scale), the white-light enhancement becomes ~0.8% of L_{star} according to the numerical modeling by Nizamov (2019).

Second, Heinzel & Shibata (2018) theoretically proposed that the contribution of flare loops to not only H α but also white-light flares can be large in the case of superflares. If this mechanism is possible, the duration and evolution could be the same since both H α and white-light radiation have the same emission source (i.e., flare loops). As in Sections 4.3 and 4.4, if the flare occurred around the limb (i.e., an “off-limb” flare), the flare loop emission can be more dominant. Because the area of flare loop is ~10% of the disk area for this superflare, the flare loop can produce the observed white-light enhancement (~0.02 of stellar luminosity) according to Heinzel & Shibata (2018), if the flare-loop density is sufficiently high (~ 10^{13} cm⁻³). The H α emission of the flare loop in the superflare case is expected to be approximately 1%–5% of the continuum level (see Wiik et al. 1996), which also corresponds well with observations.

The above two models are not supposed to be dominant in solar flares. However, our observation may indicate that they may present radiation mechanisms unique to the giant superflare.

4.5. Implications and Future Works

Section 4.4 suggests a possible radiation mechanism different from that of general solar flares. However, it is not clear from this one example alone how universal it is. More samples are needed, and the analysis of solar flares in the Sun-as-a-star view (Namekata et al. 2021) and the numerical modelings of flares (e.g., Namekata et al. 2020b) will help with interpretations. In addition, our superflare did not show a signature of a filament eruption, unlike the only previous detection of a superflare on a solar-type star (Namekata et al. 2021). It is known that in the case of the Sun, not all flares are accompanied by CMEs (Yashiro & Gopalswamy 2009), but the




CME association rates for stellar superflares are unknown. Further observations may help us estimate the frequency of filament eruptions/CMEs, which is essential information for the planetary habitability around the young Sun (see Airapetian et al. 2020) and for the estimation of a CME-related mass-loss rates (e.g., Osten & Wolk 2015).

Finally, the superflare on the solar-type star observed in this Letter is important as a proxy for a possible superflare that may occur on the present-day Sun. Interestingly, the energy of the observed superflare is comparable to the estimated upper limit of flare energy on old Sun-like stars and the present-day Sun ($\sim 4 \times 10^{34}$ erg; Okamoto et al. 2021), so the revealed properties in this Letter could be helpful to model the chromospheric radiations from a possible extreme superflare on the Sun.

The spectroscopic data presented here were obtained at the Okayama Observatory of Kyoto University, which is operated as a scientific partnership with the National Astronomical Observatory of Japan. This work and operations of OISTER were supported by the Optical and Near-infrared Astronomy Inter-University Cooperation Program and the Grants-in-Aid of the Ministry of Education. Funding for the TESS mission is provided by NASA's Science Mission Directorate. We thank S. Toriumi for discussion and comments. We acknowledge the International Space Science Institute and the supported International Team 464: The Role of Solar and Stellar Energetic Particles on (Exo) Planetary Habitability (ETERNAL, <http://www.issibern.ch/teams/exoeternal/>). Y.N. was supported by the JSPS Overseas Research Fellowship Program. This research is supported by JSPS KAKENHI grant numbers 18J20048, 21J00316 (K.N.), 17K05400, 20K04032, 20H05643 (H.M.), 21J00106 (Y.N.), 20K14521 (K.I.), and 21H01131 (K. Shibata, H.M., S.H. and D.N.).

Software: IRAF (Tody 1986), PyRAF (Science Software Branch at STScI 2012).

ORCID iDs

Kosuke Namekata  <https://orcid.org/0000-0002-1297-9485>
Hiroyuki Maehara  <https://orcid.org/0000-0003-0332-0811>
Yuta Notsu  <https://orcid.org/0000-0002-0412-0849>

References

Airapetian, V. S., Barnes, R., Cohen, O., et al. 2020, *IJAsB*, 19, 136
Aschwanden, M. J. 2019, *ApJ*, 880, 105

Aschwanden, M. J., Caspi, A., Cohen, C. M. S., et al. 2017, *ApJ*, 836, 17
Audard, M., Güdel, M., & Guinan, E. F. 1999, *ApJL*, 513, L53
Aulanier, G., Démoulin, P., Schrijver, C. J., et al. 2013, *A&A*, 549, A66
Ayres, T. R. 2015, *AJ*, 150, 7
Benz, A. O. 2017, *LRSP*, 14, 2
Emslie, A. G., Dennis, B. R., Shih, A. Y., et al. 2012, *ApJ*, 759, 71
Fausnaugh, M. M. E. A. 2020, TESS Data Release Notes: Sector 23, DR32, https://archive.stsci.edu/missions/tess/doc/tess_dm/
Guarcello, M. G., Micela, G., Sciortino, S., et al. 2019, *A&A*, 622, A210
Hao, Q., Yang, K., Cheng, X., et al. 2017, *NatCo*, 8, 2202
Hawley, S. L., & Pettersen, B. R. 1991, *ApJ*, 378, 725
Hayakawa, H., Iwahashi, K., Ebihara, Y., et al. 2017, *ApJL*, 850, L31
Heinzel, P., & Shibata, K. 2018, *ApJ*, 859, 143
Ichimoto, K., & Kurokawa, H. 1984, *SoPh*, 93, 105
Järvinen, S. P., Strassmeier, K. G., Carroll, T. A., Ilyin, I., & Weber, M. 2018, *A&A*, 620, A162
Kowalski, A. F., Hawley, S. L., Wisniewski, J. P., et al. 2013, *ApJS*, 207, 15
Kowalski, A. F., Mathioudakis, M., Hawley, S. L., et al. 2016, *ApJ*, 820, 95
Kretzschmar, M. 2011, *A&A*, 530, A84
Kurita, M., Kino, M., Iwamuro, F., et al. 2020, *PASJ*, 72, 48
Lindgren, L., Hernández, J., Bombrun, A., et al. 2018, *A&A*, 616, A2
Maehara, H., Notsu, Y., Namekata, K., et al. 2021, *PASJ*, 73, 44
Maehara, H., Notsu, Y., Notsu, S., et al. 2017, *PASJ*, 69, 41
Maehara, H., Shibayama, T., Notsu, S., et al. 2012, *Natur*, 485, 478
Maehara, H., Shibayama, T., Notsu, Y., et al. 2015, *EP&S*, 67, 59
Maldonado, J., Phillips, D. F., Dumusque, X., et al. 2019, *A&A*, 627, A118
Matsubayashi, K., Ohta, K., Iwamuro, F., et al. 2019, *PASJ*, 71, 102
Miyake, F., Nagaya, K., Masuda, K., & Nakamura, T. 2012, *Natur*, 486, 240
Namekata, K., Davenport, J. R. A., Morris, B. M., et al. 2020a, *ApJ*, 891, 103
Namekata, K., Maehara, H., Honda, S., et al. 2021, *NatAs*
Namekata, K., Maehara, H., Notsu, Y., et al. 2019, *ApJ*, 871, 187
Namekata, K., Maehara, H., Sasaki, R., et al. 2020b, *PASJ*, 72, 68
Namekata, K., Sakaue, T., Watanabe, K., et al. 2017, *ApJ*, 851, 91
Neupert, W. M. 1968, *ApJL*, 153, L59
Nizamov, B. A. 2019, *MNRAS*, 489, 4338
Notsu, Y., Maehara, H., Honda, S., et al. 2019, *ApJ*, 876, 58
Okamoto, S., Notsu, Y., Maehara, H., et al. 2021, *ApJ*, 906, 72
Osten, R. A., & Wolk, S. J. 2015, *ApJ*, 809, 79
Ricker, G. R., Winn, J. N., Vanderspek, R., et al. 2015, *JATIS*, 1, 014003
Science Software Branch at STScI 2012, PyRAF: Python alternative for IRAF, Astrophysics Source Code Library, ascl:1207.011
Şenavcı, H. V., Kılıçoğlu, T., Işık, E., et al. 2021, *MNRAS*, 502, 3343
Shibata, K., Isobe, H., Hillier, A., et al. 2013, *PASJ*, 65, 49
Shibata, K., & Magara, T. 2011, *LRSP*, 8, 6
Shibayama, T., Maehara, H., Notsu, S., et al. 2013, *ApJS*, 209, 5
Švestka, Z., Kopecký, M., & Blaha, M. 1962, *BAICz*, 13, 37
Temmer, M. 2021, *LRSP*, 18, 4
Tody, D. 1986, *Proc. SPIE*, 627, 733
Waite, I. A., Marsden, S. C., Carter, B. D., et al. 2017, *MNRAS*, 465, 2076
Wiik, J. E., Schmieder, B., Heinzel, P., & Roudier, T. 1996, *SoPh*, 166, 89
Yashiro, S., & Gopalswamy, N. 2009, in Proc. of the International Astronomical Union, IAU Symp. 257, Universal Heliophysical Processes, ed. N. Gopalswamy & D. F. Webb (Cambridge: Cambridge Univ. Press), 233